Pattern formation inside bacteria: fluctuations due to low copy number of proteins

Martin Howard[1,*] and Andrew D. Rutenberg[2]
[1] *Instituut–Lorentz, Leiden University, PO Box 9506, 2300 RA Leiden, The Netherlands and*
[2] *Department of Physics, Dalhousie University, Halifax, Nova Scotia, Canada B3H 3J5*
(Dated: February 20, 2003)

We examine fluctuation effects due to the low copy number of proteins involved in pattern–forming dynamics within a bacterium. We focus on a stochastic model of the oscillating MinCDE protein system regulating accurate cell division in *E. coli*. We find that, for some parameter regions, the protein concentrations are low enough that fluctuations are *essential* for the generation of patterns. We also examine the role of fluctuations in constraining protein concentration levels.

PACS numbers: 87.17.Ee, 87.16.Ac, 05.40.-a

In recent years, dramatic experimental progress has been made in resolving the subcellular localization of bacterial proteins. Often the proteins form self–organized, spatially inhomogeneous patterns that can involve coherent spatiotemporal oscillations. These self-organized patterns are vital for accurate cell division [1, 2, 3, 4, 5, 6, 7]. Understanding these patterns promises to reveal new mechanisms for the generation of subcellular bacterial structure. In this letter, we examine, for the first time, the impact of fluctuations on these patterns, focusing on the oscillatory MinCDE system in *E. coli* [1, 2, 3, 4, 5, 6, 7].

Each *E. coli* cell divides roughly every hour, first replicating its DNA into two nucleoids, and then dividing at midcell into two daughter cells. If division is not targeted accurately to midcell then DNA will not be distributed to both daughter cells, resulting in unviable anucleate "minicells". Division is initiated by a polymeric ring of the protein FtsZ, which forms on the inner side of the cytoplasmic membrane. Precise positioning of the FtsZ ring to midcell is controlled both by the inhibiting effect of the nucleoids ("nucleoid occlusion"), and by the MinCDE system of proteins [8]. MinC inhibits the formation of the FtsZ ring, and is recruited to the membrane by MinD. MinE is also recruited to the membrane by MinD, where it forms a dynamical ring structure that drives pole to pole oscillations of MinC and MinD, with a period of about a minute. The oscillations lead to a time–averaged midcell MinC concentration minimum [7]. As MinC inhibits FtsZ ring formation, the FtsZ can only assemble near the cell midplane. The self–organized protein patterns are thus used by the cell to obtain positional information without stationary positional markers [9, 10, 11].

Very recently, the physical principles behind the MinCDE protein patterns have been explored through reaction–diffusion equations [9, 10, 11]. The resulting equations represent protein diffusion, both in the cytoplasm and along the membrane, and also protein binding/unbinding from the cytoplasmic membrane. The slow membrane diffusion used in these models, relative to the cytoplasmic diffusion, results in Turing–like (Hopf) instabilities that spontaneously generate oscillatory patterns, in good agreement with experiment [9, 10, 11].

Bacterial proteins are, however, typically present in low numbers within the cell. This induces large fluctuations [12, 13] which have not been considered in previous pattern–forming models [9, 10, 11]. In *E. coli*, a recent assay put the copy numbers for MinD and MinE at 2000 and 1400 respectively [14]. We have therefore investigated the role of fluctuations in a discrete particle model of the *E. coli* MinCDE system where each protein molecule is explicitly tracked. This allows for a full analysis of the fluctuations of both reactions and diffusion. Although the effects of noise have been studied in subcellular models without spatial dynamics [15, 16], and also in some spatially extended patterns [17, 18, 19, 20, 21], the effects of fluctuations on *subcellular* positional information, and the constraints on protein concentrations due to fluctuations, have not previously been studied. We find that:
(i) Even at surprisingly low concentrations, the noise does not destroy the oscillatory dynamics and indeed can be vital for generating patterns in regions of parameter space where the equivalent deterministic dynamics decays away. A bacterium can thus exploit low copy number fluctuations to produce stable, self–organized patterns. This result likely applies to *any* stochastic reaction–diffusion model of pattern formation involving sufficiently few protein copies (i.e. thousands or fewer).
(ii) We find evidence that the cell employs sufficient copy numbers of the MinCDE proteins to ensure reliable midcell division; using substantially fewer copies degrades accurate positioning of the midcell MinCD minimum, using more does not lead to significantly improved accuracy.

Stochastic model. We begin by introducing the stochastic model for the MinCDE dynamics, based on our deterministic model of Ref. [9]. We employ a $1d$ discrete particle model, where the particles hop between lattice sites and where the full fluctuation effects are intrinsically included by discrete particles. As in earlier models [9, 10, 11], the MinC dynamics is omitted, since it is known to closely follow the MinD dynamics. The occupancy at site i is $n_j^{\{i\}}$, with $j = \{D, d, E, e\}$ rep-

resenting cytoplasmic MinD, membrane MinD, cytoplasmic MinE, and membrane MinE, respectively. Each protein molecule is represented as a particle which, at each timestep, may hop with equal probability $\tilde{D}_j \Delta t/(\Delta x)^2$, where Δt is the time increment, to one of its neighboring sites at $x \to x \pm \Delta x$ (except for the boundary sites at either end, where hard wall boundary conditions are imposed). At site i, the following reactions may occur, the first being for each D particle, and then for each d, E, e particle respectively:

$$\begin{array}{ll} & \text{Probability :} \\ n_D^{\{i\}} \to n_D^{\{i\}} - 1,\ n_d^{\{i\}} \to n_d^{\{i\}} + 1 & \tilde{\sigma}_1 \Delta t/(1 + \tilde{\sigma}_1' n_e^{\{i\}}) \ , \\ n_D^{\{i\}} \to n_D^{\{i\}} + 1,\ n_d^{\{i\}} \to n_d^{\{i\}} - 1 & \tilde{\sigma}_2 \, \Delta t \, n_e^{\{i\}} \ , \\ n_E^{\{i\}} \to n_E^{\{i\}} - 1,\ n_e^{\{i\}} \to n_e^{\{i\}} + 1 & \tilde{\sigma}_3 \, \Delta t \, n_D^{\{i\}} \ , \\ n_E^{\{i\}} \to n_E^{\{i\}} + 1,\ n_e^{\{i\}} \to n_e^{\{i\}} - 1 & \tilde{\sigma}_4 \Delta t/(1 + \tilde{\sigma}_4' n_D^{\{i\}}) \ . \end{array}$$

These reactions are the stochastic analogs of the reaction processes used in our deterministic partial differential equation model [9]. The $\tilde{\sigma}_1$ term describes spontaneous membrane association of MinD, whereas the $\tilde{\sigma}_2$ term describes ejection of MinD from the membrane by membrane–bound MinE. Similarly, the $\tilde{\sigma}_4$ term describes spontaneous membrane disassociation of MinE, whereas the $\tilde{\sigma}_3$ term describes recruitment of MinE to the membrane by cytoplasmic MinD. The $\tilde{\sigma}_1'$, $\tilde{\sigma}_4'$ "suppression" terms correspond to membrane MinE suppressing the binding of MinD to the membrane, and to cytoplasmic MinD suppressing the unbinding of membrane MinE.

ATP dynamics. We next address the question of how ATP dynamics fits into the model. Experimentally, MinD is an ATPase [22] and it is the MinD-ATP complex that binds to the membrane, whereas the release of MinD back into the cytoplasm requires MinE–induced ATP hydrolysis [23]. Our model assumes that, following ATP hydrolysis and release of MinD into the cytoplasm, nucleotide exchange is sufficiently rapid to allow for membrane reattachment of MinD-ATP almost immediately. As a result, we only model MinD-ATP in the cytoplasm ($n_D^{\{i\}}$) and on the membrane ($n_d^{\{i\}}$). Like "actin treadmilling" in eukaryotic cells, the ATP driven binding and unbinding of MinD allows for a cyclic MinCDE pattern to be maintained with only low levels of protein synthesis: *this makes the pattern–forming dynamics extremely energy efficient.* This recycling is also consistent with experiments where protein synthesis was blocked, but where the MinCDE oscillations were observed to continue unaffected [1]. Consequently, the above model (similar to that of Ref. [11]) does not include protein synthesis or degradation. These processes occur, but on longer time scales than the relatively rapid MinCDE oscillations.

Simulations. In our stochastic model simulations, we use time and spatial increments $\Delta x = 0.02\ \mu m$, $\Delta t = 2 \times 10^{-5}\ s$, so that 100 lattice sites model a 2 μm bacterium. We use: $\tilde{D}_D = 0.28\ \mu m^2\ s^{-1}$, $\tilde{D}_d = 0.003\ \mu m^2\ s^{-1}$, $\tilde{D}_E = 0.6\ \mu m^2\ s^{-1}$, $\tilde{D}_e = 0.006\ \mu m^2\ s^{-1}$, $\tilde{\sigma}_1 = 20\ s^{-1}$, and $\tilde{\sigma}_4 = 0.8\ s^{-1}$. Note that the membrane diffusion constants are much smaller than those in the cytoplasm; this agrees with recent data indicating that MinD may polymerize on the membrane [23, 24]. For the remaining variables of the model, we focus on 4 representative parameter sets shown in Table I, where we define N as the total number of MinD proteins, equal to the total number of MinE proteins [25]. However, we emphasize that our results for the oscillatory behavior observed below are typical for large regions of parameter space. Initially, MinD and MinE particles are randomly distributed on the membrane and in the cytoplasm. Equal numbers of proteins are used since "wild–type" oscillations are observed when both proteins are equally expressed on plasmids (this is consistent, within experimental uncertainties, with the earlier quoted MinDE assay [14]).

Fluctuation driven instability. Using the parameters in Table I, we find that the presence of noise is vital for the oscillations to persist. This is shown in Fig. 1, where the ratio of the average MinD density in the right–hand 30% of the cell to that in the left–hand 30% of the cell is plotted as a function of time for the stochastic model (at $N = 200$ and $N = 1500$) and for the deterministic model [9] with equivalent parameters (i.e. with the above reaction probabilities directly transformed into deterministic reaction rates). In both cases, for the deterministic model, the protein concentrations rapidly decay away to the homogeneous steady state (in agreement with linear stability analysis [9]), whereas regular oscillations continue for the stochastic model. Hence the average behavior of the stochastic model is clearly not describable using the naively equivalent deterministic model. To investigate this issue in more detail, we have examined how steady–state/oscillation bifurcations in the deterministic model are altered in the stochastic model. As a representative example, at $N = 1500$, using the above parameter set in the stochastic model, but with $\tilde{D}_d = 0.001\ \mu m^2\ s^{-1}$, $\tilde{D}_e = 0.003\ \mu m^2\ s^{-1}$, $\tilde{\sigma}_1' = 0.2$ and varying $\tilde{\sigma}_4$, we find that the transition from oscillatory to steady–state behavior is reduced by around 40% from $\tilde{\sigma}_4 = 0.63\ s^{-1}$ (deterministic) to $\tilde{\sigma}_4 \approx 0.39\ s^{-1}$ (stochastic), as determined using the end to end MinD ratio. The noise does smear out the transition somewhat in the stochastic model (the transition at $\tilde{\sigma}_4 \approx 0.39\ s^{-1}$ has width $\pm 0.05\ s^{-1}$), but this effect is rather small. Hence this smearing out cannot account for the large regions of parameter space where oscillations occur in the stochastic, but not the deterministic, model. Rather, we have a fluctuation driven instability, where the noise has shifted the location of the transition, thereby promoting oscillations in large regions of parameter space where it would be forbidden in the equivalent deterministic model (see Fig. 1). *Cells can in principle exploit low copy number fluctuations to generate pattern–forming dynamics.* The oscillations continue down to very low concentrations

N	$\tilde{\sigma}_1'$	$\tilde{\sigma}_2$ (s^{-1})	$\tilde{\sigma}_3$ (s^{-1})	$\tilde{\sigma}_4'$
200	25.0	0.27	30.0	20.0
400	2.0	0.135	15.0	10.0
800	0.6	0.0675	7.5	5.0
1500	0.25	0.036	4.0	2.7

TABLE I: Reaction rate parameter values.

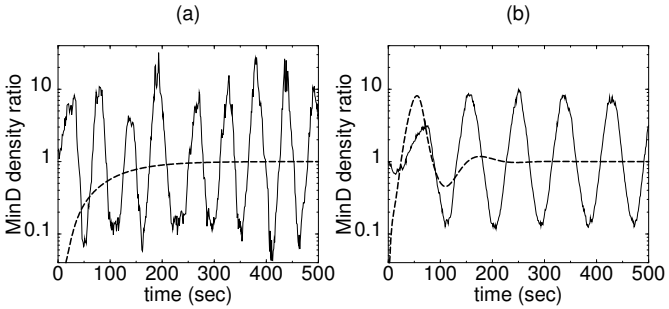

FIG. 1: Ratio of average MinD density in right–hand 30% of the cell to that in left–hand 30%. Full line: stochastic dynamics with random initial conditions at (a) $N = 200$ (b) $N = 1500$; dashed line: deterministic dynamics with equivalent parameters but with inhomogeneous initial conditions.

($N = 200$), underlining the robustness of the dynamics.

The above examples show that the fluctuations are often essential for pattern formation. However, it also possible for the stochastic and deterministic models with equivalent parameters [9] both to generate oscillations. Hence we cannot definitively conclude that fluctuations are essential for the MinCDE oscillations. Nevertheless, our analysis does show conclusively that cells can exploit low copy number fluctuations for the generation of dynamical subcellular structure.

Effect of fluctuations on the midcell MinD minimum. In Fig. 2, we plot the MinD and MinE concentration profiles for $N = 200$ and $N = 1500$, showing their averages over 160 and 110 successive cycles, respectively, and also for 4 individual data sets each, where each set is averaged over only an *individual* oscillation cycle. For the long time data sets, we find that the midcell MinD concentration minimum (and a MinE concentration maximum) are still robustly reproduced even in the presence of noise. However, as can be seen from the data averaged over individual cycles, the fluctuations around this average can be very large for small N. In Fig. 3 we show histograms of the position of the MinD concentration minimum, where each minimum is determined over a single oscillation cycle (the use of a single cycle here is explained below). For $N = 1500$, the histogram is sharply peaked around the cell center at 1.0 ± 0.07 μm (1 standard deviation). As expected, with decreasing N the width increases: 0.09 μm at $N = 800$, 0.16 μm at $N = 400$, and 0.27 μm at $N = 200$ [25]. The width of the midcell localization is large, particularly at protein counts ($N = 200$ and $N = 400$) that are significantly below those seen naturally. Hence, using significantly fewer protein copies degrades the accuracy of midcell division.

Nucleoids, when present, also affect the positioning of the FtsZ ring through the poorly understood phenomenon of "nucleoid occlusion" [8], where FtsZ rings do not nucleate over nucleoids and are restricted to either near the midcell or at the cell poles. Segregated nucleoids (at the 1/4 and 3/4 positions along the cell) will truncate the tails of the distributions shown in Fig. 3, further enhancing the accuracy of midcell division (in agreement with experiment [8, 26]). In normal cells with nucleoids, it is particularly important that the MinCDE system block polar FtsZ rings, since the nucleoids themselves will inhibit FtsZ rings elsewhere away from midcell. Assuming that FtsZ nucleation occurs at a single cycle MinD minimum (see below), then from Fig. 3 we see that $N = 1500$ is a high enough concentration to reduce the probability of polar division to considerably less than 0.01 per oscillation cycle. Given that about 50 complete oscillation cycles normally occur between successive divisions, we see that attaining this level of accuracy is important. Significantly lower concentrations than $N = 1500$ will lead to an unacceptable probability of polar division, while higher concentrations will lead to only marginally increased accuracy, but at the cost of manufacturing many additional protein copies. From these simple arguments based on fluctuation effects, we see that *E. coli* may be using an optimal number of Min proteins, trading off midpoint precision against the cost of protein synthesis. There will be other constraints on the protein copy numbers (e.g., sufficient MinC to successfully inhibit off–center FtsZ ring formation), but fluctuations set useful bounds on the concentration levels.

Comparison with experiment. Experimentally, the precision of the MinCDE system can be probed in anucleate cells by measuring the position of the FtsZ ring. In these cells the only positional guide for division is the MinCDE system, which functions even in the absence of the nucleoids. Indeed in these anucleate cells the FtsZ ring position is placed at midcell with a width of 0.12 μm (scaled to a 2 μm length) [8], somewhat larger than the MinD distribution width 0.07 μm at $N = 1500$. We would expect that FtsZ ring nucleation would not precisely track the MinCD minimum, which could account for the difference. In order to make this comparison we need to know how many cycles the FtsZ nucleation averages over to identify the location of the MinD minimum. Experimentally, this timescale is on the order of a minute, since, from Ref. [1], oscillation cycles of between 30 s and 120 s give normal division. As referred to earlier, this justifies a rough comparison of the width of the single cycle (~ 90 s) MinD density minimum distribution at $N = 1500$ with that of the FtsZ distribution in anucleate cells.

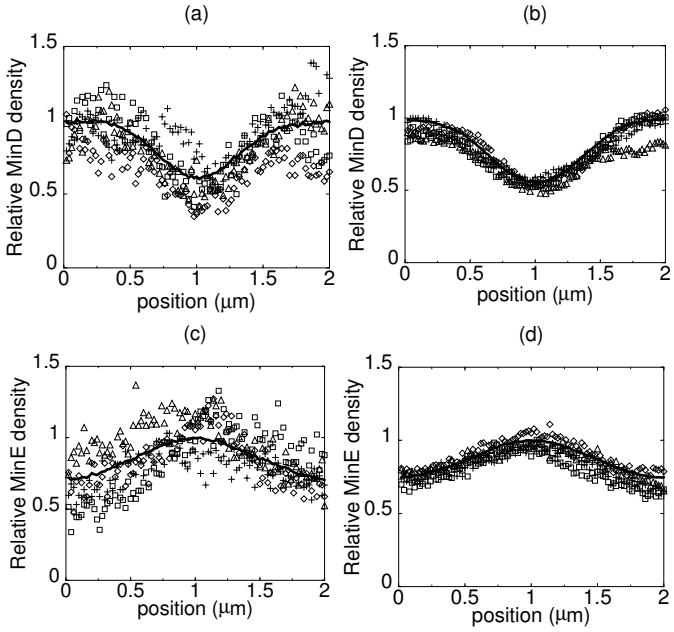

FIG. 2: (a,b) MinD and (c,d) MinE relative density profiles in stochastic model with (a,c) $N = 200$ (b,d) $N = 1500$. Thick lines represent averages over (a,c) 160 and (b,d) 110 consecutive cycles respectively (maximum average density normalized to unity). Symbols $(+, \diamond, \triangle, \Box)$ represent individual data sets that are averaged only over a single oscillation cycle.

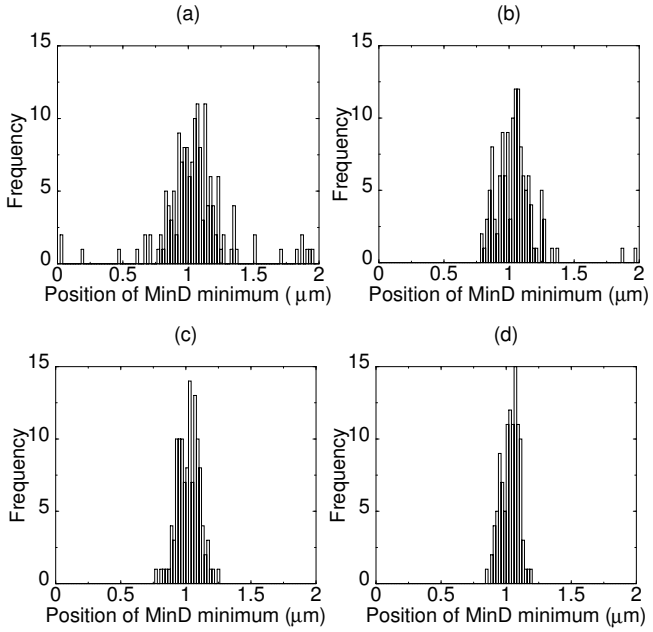

FIG. 3: Histogram for position of MinD density minimum in the stochastic model with (a) $N = 200$, (b) $N = 400$, (c) $N = 800$, (d) $N = 1500$. The position of each minimum is computed by averaging over a single oscillation cycle. Data is for 160, 135, 120 and 110 consecutive cycles respectively.

In conclusion, we have studied fluctuations in the *E. coli* MinCDE system. In some regimes, we have found that fluctuations are *essential* for pattern generation. We have also found evidence that the MinCDE concentrations may be optimal for reliable midcell division. Based on the MinCDE system, we see that $O(10^3)$ copies of pattern forming proteins are required in bacteria to obtain positional information accurate to within a few percent.

We acknowledge useful conversations with P. de Boer, M. van Hecke, K. Kruse, J. Lutkenhaus, and S. de Vet. M.H. acknowledges financial support from Stichting FOM and from The Royal Society. A.D.R acknowledges financial support from NSERC Canada.

*Present address: Department of Mathematics, Imperial College London, South Kensington Campus, London SW7 2AZ, U.K.

[1] D. M. Raskin and P. A. J. de Boer, Proc. Natl. Acad. Sci. U.S.A. **96**, 4971 (1999).
[2] D. M. Raskin and P. A. J. de Boer, J. Bacteriol. **181**, 6419 (1999).
[3] Z. Hu and J. Lutkenhaus, Mol. Microbiol. **34**, 82 (1999).
[4] S. L. Rowland *et al.*, J. Bacteriol. **182**, 613 (2000).
[5] X. Fu *et al.*, Proc. Natl. Acad. Sci. U.S.A. **98**, 980 (2001).
[6] L. I. Rothfield *et al.*, Cell **106**, 13 (2001).
[7] C. A. Hale *et al.*, EMBO J. **20**, 1563 (2001).
[8] X.-C. Yu and W. Margolin, Mol. Microbiol. **32**, 315 (1999).
[9] M. Howard, A. D. Rutenberg, and S. de Vet, Phys. Rev. Lett. **87**, 278102 (2001).
[10] H. Meinhardt and P. A. J. de Boer, Proc. Natl. Acad. Sci. U.S.A. **98**, 14202 (2001).
[11] K. Kruse, Biophys. J. **82**, 618 (2002).
[12] H. H. McAdams and A. Arkin, Trends Genet. **15**, 65 (1999).
[13] W. Bialek, in *Advances in Neural Information Processing 13*, edited by T. K. Leen, T. G. Dietterich, and V. Tresp (MIT Press, Cambridge, 2001), p. 103.
[14] Y.-L. Shih *et al.*, EMBO J. **21**, 3347 (2002).
[15] J. Paulsson *et al.*, Proc. Natl. Acad. Sci. U.S.A. **97**, 7148 (2000).
[16] J. M. G. Vilar *et al.*, Proc. Natl. Acad. Sci. U.S.A. **99**, 5988 (2002).
[17] D. A. Kessler and H. Levine, Nature **394**, 556 (1998).
[18] M. Falcke *et al.*, Phys. Rev. E **62**, 2636 (2000).
[19] J. M. G. Vilar and J. M. Rubí, Phys. Rev. Lett. **78**, 2886 (1997); Physica A **277**, 327 (2000).
[20] J. García–Ojalvo and J. M. Sancho, *Noise in Spatially Extended Systems* (Springer–Verlag, New York, 1999).
[21] H. Zhonghuai *et al.*, Phys. Rev. Lett. **81**, 2854 (1998).
[22] P. A. J. de Boer *et al.*, EMBO J. **10**, 4371 (1991).
[23] Z. Hu *et al.*, Proc. Natl. Acad. Sci. U.S.A. **99**, 6761 (2002).
[24] We have also simulated a stochastic $1d$ model where membrane MinD can polymerize and is then permitted to unbind only from polymer ends. Using a large membrane diffusion constant $0.1\mu m^2 s^{-1}$ for unpolymerized membrane MinD, zero diffusion for polymerized MinD, and otherwise unchanged parameters, we again recover oscillatory dynamics, with an average midcell MinD concentration minimum. Thus, the key feature introduced by the polymerization is the small membrane diffusivity.
[25] As N is scaled, so must the reaction rates in order to maintain the same equivalent deterministic model. This

ensures that the variation in widths is primarily due to changes in fluctuations (induced by varying N), and not to changes in the membrane binding/unbinding rates.

[26] Q. Sun *et al.*, Mol. Microbiol. **29**, 491 (1998).